SOLUTION OF INTEGRO-DIFFERENTIAL EQUATIONS USING MATHEMATICA WITH APPLICATION IN FRACTURE MECHANICS *

Marin Marinov
Computer Science Department, New Bulgarian University
Sofia 1618, Bulgaria, E-mail: mlmarinov@nbu.bg,
Tsviatko Rangelov
Institute of Mathematics and Informatics, Bulgarian Academy of Sciences
Sofia 1113, Bulgaria, E-mail: rangelov@math.bas.bg,

ABSTRACT

Integro-differential equations for anti-plane cracks in functionally graded piezoelectric solid in a frequency domain are solved by using Mathematica. Exponential variation of the material parameters is considered. The numerical solution provides crack opening displacement from which the generalized stress intensity factor is determined. A validation and a parametric study is presented to demonstrate the accuracy of the solution and its dependance on the dynamic load.

Key words. Functionally graded piezoelectric solid, Anti-plane cracks, Integro-differential equations, Stress intensity factor
Math. Subj. Class. 74E05, 74F15, 74S15, 74H35

1 Introduction

Numerical solution of integro-differential equations (IDE) for coupled problems like piezoelectric system is a tool for fracture mechanics models. The importance of investigation of functionally graded piezoelectric materials (FGPM) is due to their application in transducers, actuators, wave generators and other smart intelligent systems. During the manufacturing process and also in service conditions cracks and other defects can appear that cause failure of these devises. There are mainly two semi-analytical numerical methods for studying of the elastodynamic problems in inhomogeneous domains. One of them is the dual integral equation method, see [4], [3], [8], [9] and [12], where anti-plane line cracks in domains with exponentially varying properties in parallel or perpendicular direction to the

*Proceedings of the 6^{th} ICCSE 2010, Eds. R Stainov, V. Kanabar, P. Assenova, pp. 158-167, 2010, ISBN 978-954-535-573-8.

crack line is studied. The boundary value problem (BVP) is transformed to a dual integral equations on the crack line and SIF is obtained as a solution of a suitable Fredholm integral equation. Other method is boundary integral equation method (BIEM) treated in [5] and [11], where arbitrary shaped anti-plane cracks in domains with quadratic, sinusoidal or exponential inhomogeneity is investigated. The BVP is transformed to an equivalent IDE on the crack and crack opening displacement (COD) is found using BIEM. In this case the solution can be obtained in every point of the domain, together with the stress intensity factor (SIF) - the leading coefficient in the asymptotic of the solution near the crack edges.

The aim of the work is to solve an IDE for anti-plane cracked FGPM with exponentially varying properties. Fundamental solution obtained by using the Radon transform is implemented in the created by Mathematica software numerical code. The applicability of the method is demonstrated by numerical examples.

2 Statement of the problem

We consider a piezoelectric plane with an arbitrary shaped finite crack $S_{cr} = S_{cr}^{+} \cup S_{cr}^{-}$ - an open arc, poled in x_3 - direction and subjected to time-harmonic loading.

The mechanical and electrical loading is assumed to be such that the only nonvanishing displacements are the anti-plane mechanical displacement $u_3(x,t)$ and the in-plane electrical displacements $D_i = D_i(x,t)$, $i = 1, 2$, $x = (x_1, x_2)$. Since all fields are time-harmonic with the frequency ω the common multiplier $e^{i\omega t}$ is suppressed here and in the following. For such a case, assuming quasi-static approximation of piezoelectricity, the field equation in absence of body force is given by the balance equation

$$\sigma_{i3,i} + \rho\omega^2 u_3 = 0, \quad D_{i,i} = 0, \tag{1}$$

the strain - displacement and electric field - potential relations

$$s_{i3} = u_{3,i}, \quad E_i = -\Phi_{,i}, \tag{2}$$

and the constitutive relations, see [7]

$$\begin{aligned} \sigma_{i3} &= c_{44} s_{i3} - e_{15} E_i, \\ D_i &= e_{15} s_{i3} + \varepsilon_{11} E_i. \end{aligned} \tag{3}$$

The subscript $i = 1, 2$ and comma denotes partial differentiation. Here σ_{i3}, s_{i3}, E_i, Φ are the stress tensor, strain tensor, electric field vector and electric potential, respectively. Furthermore, $\rho(x) > 0$, $c_{44}(x) > 0$, $\varepsilon_{11}(x) > 0$ are the inhomogeneous mass density, the shear stiffness, piezoelectric and dielectric permittivity characteristics. Introducing (3) and (2) into (1) leads to the coupled system

$$\begin{aligned} &(c_{44} u_{3,i})_{,i} + (e_{15}\Phi_{,i})_{,i} + \rho\omega^2 u_3 = 0, \\ &(e_{15} u_{3,i})_{,i} - (\varepsilon_{11}\Phi_{,i})_{,i} = 0. \end{aligned} \tag{4}$$

where the summation convention over repeated indices is applied. The basic equations can be written in a more compact form if the notation $u_J = (u_3, \Phi)$, $J = 3, 4$ is introduced. The constitutive equations (3) then take the form

$$\sigma_{iJ} = C_{iJKl} u_{K,l}, \quad i, l = 1, 2, \tag{5}$$

where $C_{i33l} = \begin{cases} c_{44}, i = l \\ 0, \quad i \neq l \end{cases}$, $C_{i34l} = \begin{cases} e_{15}, i = l \\ 0, \quad i \neq l \end{cases}$, $C_{i44l} = \begin{cases} -\varepsilon_{11}, i = l \\ 0, \quad\quad i \neq l \end{cases}$ and equation (4) is reduced to

$$\sigma_{iJ,i} + \rho_{JK}\omega^2 u_K = 0, \quad J, K = 3, 4, \tag{6}$$

where $\rho_{JK} = \begin{cases} \rho, J = K = 3 \\ 0, J = 4 \text{ or } K = 4 \end{cases}$.

Along the crack line it is supposed

$$t_J = 0 \quad \text{on } S_{cr}, \tag{7}$$

where $t_J = \sigma_{iJ}n_i$ and $n = (n_1, n_2)$ is the outer normal vector to S^+_{cr}. The boundary condition (7) means that the crack faces are free of mechanical traction as well as of surface charge, i.e. the crack is electrically impermeable.

We further assume that the mass density and material parameters vary in the same manner with x, through function $h(x) = e^{2\langle a,x\rangle}$, where $\langle .,. \rangle$ means the scalar product in R^2, and $a = (a_1, a_2)$, such that

$$c_{44}(x) = c^0_{44}h(x), \quad e_{15}(x) = e^0_{15}h(x), \quad \varepsilon_{11}(x) = \varepsilon^0_{11}h(x), \quad \rho(x) = \rho^0 h(x). \tag{8}$$

One way to solve the problem (6), (7) numerically is to transform it into the equivalent integro-differential equation along the crack S_{cr}. This can be done if we are able to use an appropriate fundamental solution for the equation (6).

3 Fundamental solution and free field solution

3.1 Fundamental solution

The fundamental solution of the equation (6) is defined as solution of the equation

$$\sigma^*_{iJM,i} + \rho_{JK}\omega^2 u^*_{KM} = -\delta_{JM}\delta(x, \xi), \tag{9}$$

where $\sigma^*_{iJK} = C_{iJMl}u^*_{KM,l}$, $J, K, M = 3, 4$, $i, l = 1, 2$, δ is the Dirac function, $x = (x_1, x_2)$, $\xi = (\xi_1, \xi_2)$ and δ_{JM} is the Kronecker symbol. For the considered inhomogeneity function $h(x)$ the fundamental solution is obtained in [10] as follows. First the equation (9) is transformed by a suitable change of functions to an equation with constant coefficients. In a second step we apply Radon transform which allows the construction of a set of fundamental solutions depending on the roots of the characteristic equation of the obtained ODE-system. Finally, using both the inverse Radon transform and the inverse change of functions, the fundamental solutions of equation (6) is obtained in a closed form. In the first step the smooth transformation $u^*_{KM} = h^{-1/2}U^*_{KM}$ applied to (9) gives

$$C^0_{iJKi}U^*_{KM,ii} + [\rho^0_{JK}\omega^2 - C^0_{iJKi}a^2_i]U^*_{KM} = h^{-1/2}(\xi)\delta_{JM}\delta(x, \xi). \tag{10}$$

To solve the equation (10) we use the Radon transform, see Zayed [16]. In R^2 it is defined for the set $f \in \Im$ of rapidly decreasing C^∞ functions is defined as, , $\hat{f}(s, m) = R[f(x)] = \int_{\langle m,x\rangle=s} f(x)dx = \int f(x)\delta(s - \langle m, x\rangle)dx$ with the inverse transform $f(x) = \frac{1}{4\pi^2}\int_{|m|=1} K(\hat{f}(s, m)|_{s=\langle m,x\rangle}dm$, $K(\hat{f}) = \int_{-\infty}^{\infty} \frac{\partial_\sigma \hat{f}(\sigma,m)}{s-\sigma}d\sigma$. Applying the Radon transform to both sides of (10) we get with $p_{JK} = C^0_{iJKi}a^2_i$

$$[C^0_{iJKi}m^2_i\partial^2_s + (\rho^0_{JK}\omega^2 - p_{JK})]\hat{U}^*_{KM} = -h_{-1/2}(\xi)\delta_{JM}\delta(s - \langle\xi, m\rangle), \tag{11}$$

These two systems of two linear second order ordinary differential equations are solved following [13]. Denote $\gamma = (\rho^0\omega^2 - a_0 p)a_0^{-1}$, $a_0 = c_{44}^0 + \frac{e_{15}^{02}}{\varepsilon_{11}^0}$, $\omega_0 = \sqrt{\frac{a_0}{\rho^0}}|a|$. Due to the frequency ω we obtain the solutions of (11) as follows:

(i) $\gamma > 0$, i.e. $\omega > \omega_0$, $k = \sqrt{\gamma}$,

$$\begin{aligned} &\hat{U}_{33}^* = h^{-1/2}(\xi)\tfrac{i}{2ka_0}e^{ik|s-\tau|}, \quad \hat{U}_{34}^* = h^{-1/2}(\xi)\tfrac{i}{2ka_0}\tfrac{e_{15}^0}{\varepsilon_{11}^0}e^{ik|s-\tau|} \\ &\hat{U}_{43}^* = \hat{U}_{34}^*, \quad \hat{U}_{44}^* = h^{-1/2}(\xi)[\tfrac{i}{2ka_0}(\tfrac{e_{15}^0}{\varepsilon_{11}^0})^2 e^{ik|s-\tau|} + \tfrac{1}{\varepsilon_{11}^0}\tfrac{1}{2|a|}e^{|a||s-\tau|}]; \end{aligned} \tag{12}$$

(ii) $\gamma = 0$, i.e. $\omega = \omega_0$

$$\begin{aligned} &\hat{U}_{33}^* = -h^{-1/2}(\xi)\tfrac{1}{2a_0}|s-\tau|, \quad \hat{U}_{34}^* = -h^{-1/2}(\xi)\tfrac{1}{2a_0}\tfrac{e_{15}^0}{\varepsilon_{11}^0}|s-\tau| \\ &\hat{U}_{43}^* = \hat{U}_{34}^*, \quad \hat{U}_{44}^* = -h^{-1/2}(\xi)[\tfrac{1}{2a_0}(\tfrac{e_{15}^0}{\varepsilon_{11}^0})^2|s-\tau|]. \end{aligned} \tag{13}$$

(iii) $\gamma < 0$, i.e. $\omega < \omega_0$, $k = \sqrt{|\gamma|}$,

$$\begin{aligned} &\hat{U}_{33}^* = -h^{-1/2}(\xi)\tfrac{1}{2ka_0}e^{k|s-\tau|}, \quad \hat{U}_{34}^* = -h^{-1/2}(\xi)\tfrac{1}{2ka_0}\tfrac{e_{15}^0}{\varepsilon_{11}^0}e^{k|s-\tau|} \\ &\hat{U}_{43}^* = \hat{U}_{34}^*, \quad \hat{U}_{44}^* = -h^{-1/2}(\xi)[\tfrac{1}{2ka_0}(\tfrac{e_{15}^0}{\varepsilon_{11}^0})^2 e^{k|s-\tau|} - \tfrac{1}{\varepsilon_{11}^0}\tfrac{1}{2|a|}e^{|a||s-\tau|}]. \end{aligned} \tag{14}$$

In order to obtain the fundamental solution we finally have to apply inverse Radon transform to $\hat{U}_{KJ}^*$. Since the functions $\hat{U}_{KJ}^*$ are linear combinations of $e^{iq|s-\tau|}$, $e^{q|s-\tau|}$ and $|s-\tau|$, for the first part of the inverse Radon transform the formulas

$$\begin{aligned} &K(e^{iq|s-\tau|}) = -iq\{i\pi e^{iq\beta} - 2[\mathrm{ci}(q\beta)\cos(q\beta) + \mathrm{si}(q\beta)\sin(q\beta)]\}|_{\beta=|s-\tau|}, \\ &K(e^{q|s-\tau|}) = q\{2[\mathrm{chi}(q\beta)\cosh(q\beta) - \mathrm{shi}(q\beta)\sinh(q\beta)]\}|_{\beta=|s-\tau|}, \\ &K(|s-\tau|) = 2\ln\beta|_{\beta=|s-\tau|}, \end{aligned} \tag{15}$$

are used where $\mathrm{ci}(\eta) = -\int_\eta^\infty \frac{\cos t}{t}dt$, $\mathrm{si}(\eta) = -\int_\eta^\infty \frac{\sin t}{t}dt$ are the cosine integral and sine integral functions and $\mathrm{chi}(\eta) = -\int_0^\eta \frac{\cosh t - 1}{t}dt + \ln\eta + C$, $\mathrm{shi}(\eta) = -\int_0^\eta \frac{\sinh t}{t}dt$ are the hyperbolic cosine and sine integral functions with Euler's constant C, see Bateman and Erdelyi [2].

After having obtained $\hat{U}_{KJ}^*$ by completing inverse Radon transforms the final form of the fundamental solution is derived from the smooth transformation.

3.2 Free field solution

We are asking for a solution of Eq. (6) of the form

$$\begin{aligned} &u(x,\eta) = h^{-1/2}(x)U(x,\eta) = h^{-1/2}pe^{ik<x,\eta>}, \\ &p = (p_1,p_2), \eta = (\eta_1,\eta_2), |\eta| = 1, \end{aligned} \tag{16}$$

where p is a polarization vector, k is wave number and η is a direction of the incident wave. Again there are three cases with respect to ω.

(i) $\omega > \omega_0$. In this case $k = \pm\sqrt{\frac{\rho^0\omega^2}{a_0} - |a|^2}$, the corresponding polarization vector is $p = (1, \frac{e_{15}^0}{\varepsilon_{11}^0})$ and

$$\begin{aligned} &u(x,\eta) = e^{-<a,x>}\begin{pmatrix} 1 \\ \frac{e_{15}^0}{\varepsilon_{11}^0} \end{pmatrix} e^{ik<x,\eta>} \\ &t_3(x,\eta)|_{S_{cr}} = a_0 < ik\eta - a, n > e^{<a+ik\eta,x>}, t_4(x,\eta)|_{S_{cr}} = 0. \end{aligned} \tag{17}$$

(ii) $\omega = \omega_0$. In this case $k = 0$, the corresponding polarization vector is $p = (1, \frac{e^0_{15}}{\varepsilon^0_{11}})$ and

$$\begin{array}{l} u(x,\eta) = e^{-<a,x>}\left(\begin{array}{c} 1 \\ \frac{e^0_{15}}{\varepsilon^0_{11}} \end{array}\right) \\ t_3(x,\eta)|_{S_{cr}} = -a_0 < a, n > e^{<a,x>}, t_4(x,\eta)|_{S_{cr}} = 0. \end{array} \tag{18}$$

(iii) $\omega < \omega_0$. In this case $k = \pm i\sqrt{|\frac{\rho^0\omega^2}{a_0} - |a|^2|}$, the corresponding polarization vector is $p = (1, \frac{e^0_{15}}{\varepsilon^0_{11}})$ and

$$\begin{array}{l} u(x,\eta) = e^{-<a,x>}\left(\begin{array}{c} 1 \\ \frac{e^0_{15}}{\varepsilon^0_{11}} \end{array}\right) e^{|k|<x,\eta>} \\ t_3(x,\eta)|_{S_{cr}} = a_0 < |k|\eta - a, n > e^{<a+|k|\eta,x>}, t_4(x,\eta)|_{S_{cr}} = 0. \end{array} \tag{19}$$

4 Non-hypersingular BIEM

The non-hypersingular traction based BIE is derived following the procedure given by [6] and [15] . Using superposition principle the displacements and the traction are represented as $u_J = u^{in}_J + u^{sc}_J$, $t_J = t^{in}_J + t^{sc}_J$ where u^{in}_J, t^{in}_J is the free field solution and its traction on S_{cr} derived in section 3.2. From the boundary condition (7) we have $t^{sc}_J = -t^{in}_J$ on S_{cr}. Let us introduce the smooth change of functions

$$u_J(x,\omega) = e^{-<a,x>}W_J(x,\omega). \tag{20}$$

and suppose that $W_J(x,\omega)$ satisfies Sommerfeld-type condition on infinity, more specifically

$$W_3 = o(|x|^{-1}), W_4 = o(e^{-|a||x|}) \quad \text{for} \quad |x| \to \infty. \tag{21}$$

Condition (21) ensure uniqueness of the scattering field u^{sc}_J for a given incident field u^{in}_J. Following Akamatsu and Nakamura [1] it can be proved that the boundary value problem (BVP) (6), (7) admit continuous differentiable solutions.

For u_J, u^*_{JK} we apply the Green formula in the domain $\Omega_R \setminus \Omega_\varepsilon$, Ω_R is a disk with large radius R and Ω_ε is a small neighborhood of S_{cr}. Applying the representation formulae for the generalized displacement gradient $u_{K,l}$, see [15] an integro-differential equation on $\partial\Omega_R \cup \partial\Omega_\varepsilon$ is obtained. Using the condition (20) integrals over $\partial\Omega_R$ go to 0 for $R \to \infty$. Taking the limit $\varepsilon \to 0$, i.e. $x \to S_{cr}$ and using the boundary condition (7), i.e. $t^{sc}_J = -t^{in}_J$ on S_{cr} the following system of BIE is equivalent to the BVP (6), (7)

$$\begin{array}{l} -t^{in}_J(x) = C_{iJKl}n_i(x)\displaystyle\int_{S_{cr}}[(\sigma^*_{\eta PK}(x,y)\Delta u_{P,\eta}(y) - \rho_{QP}\omega^2 u^*_{QK}(x,y)\Delta u_P(y))\delta_{\lambda l} \\ -\sigma^*_{\lambda PK}(x,y)\Delta u_{P,l}(y)]n_\lambda(y)dS, \quad x \in S_{cr} \end{array} \tag{22}$$

Here, u^*_{JK} is the fundamental solution of (9), derived in section 3.1, $\sigma^*_{iJQ} = C_{iJKl}u^*_{KQ,l}$ is the corresponding stress, and $\Delta u_J = u_J|_{S^+_{cr}} - u_J|_{S^-_{cr}}$ is the generalized COD. Equation (22) constitute a system of integro-differential equations for the unknown Δu_J on the crack line S_{cr}. From its solution the generalized displacement u_J at every internal point of the plane can be determined by using the corresponding representation formulae, see [11].

5 Numerical realization and results

5.1 Numerical realization

The numerical procedure for the solution of the boundary value problem follows the numerical algorithm developed and validated in [6] and [11]. The crack S_{cr} is discretized by quadratic boundary elements (BE) away from the crack-tips and special crack-tip quarter-point BE near the crack-tips to model the asymptotic behavior of the displacement and the traction. Applying the shifted point scheme, the singular integrals converge in Cauchy principal value (CPV) sense, since the smoothness requirements $\Delta u_J \in C^{1+\alpha}(S_{cr})$ of the approximation are fulfilled. Due to the form of the fundamental solution as an integral over the unit circle, all integrals in Eq. (22) are two dimensional. In general there appear two types of integrals - regular integrals and singular integrals, the latter including a weak "$\ln r$" type singularity and also a strong "$\frac{1}{r}$" type singularity. The regular integrals are solved using quasi Monte Carlo method, while the singular integrals are solved with a combined method - partially analytically as CPV integrals.

After the discretization procedure an algebraic linear complex system of equations is obtained and solved. The program code based on Mathematica has been created following the above outlined procedure.

The mechanical dynamic SIF K_{III}, the electrical displacement intensity factor K_D and the electric intensity factor K_E are obtained directly from the traction nodal values ahead of the crack-tip. For example, in case of a straight crack, the interval $(-c, c)$ on the Ox_1 axis, the expressions are

$$\begin{array}{ll} K_{III} = \lim_{x_1 \to \pm c} t_3 \sqrt{2\pi(x_1 \mp c)}, & K_D = \lim_{x_1 \to \pm c} t_4 \sqrt{2\pi(x_1 \mp c)}, \\ K_E = \lim_{x_1 \to \pm c} E_3 \sqrt{2\pi(x_1 \mp c)}, & E_3 = \frac{e_{15}}{e_{15}^2 + c_{44}\varepsilon_{11}}(-e_{15}t_3 + c_{44}t_4), \end{array} \tag{23}$$

where t_J is the generalized traction at the point $(x_1, 0)$ close to the crack-tip.

Mathematic's code consists of the following parts:

(i) Definition of the material parameters, crack geometry, BE and quadratic approximation;

(ii) Definition of the fundamental solution, its derivatives and the asymptotic for small arguments;

(iii) Definition of the integro-differential equations and the anti-plane load;

(iv) Solution of the integrals and forming the system of linear equations for the unknowns COD;

(v) Solution of the linear system;

(vi) Formulae for the solution in every point of the plane;

(vii) Evaluation of the SIF - the leading coefficients in the asymptotic of the solution near the crack edges.

The main points in the solution procedure are (iv) and (v). In (iv) the integrals over the BE are two-dimensional (in the intrinsic coordinates in the domain $(z, \varphi) \in [-1, 1] \times [0, 2\pi]$) with regular and singular kernels: with weak singularity as $O(\log r)$ and with strong singularities $O(1/r)$. The regular integrals are solves using AdaptiveMonteCarlo Method with 300 points. The singular integrals are solved analytically with respect to r and numerically with respect to φ, and due to their oscillatory behaviour they are treated as 0.5 by two dimensional integral and solved again with AdaptiveMonteCarlo Method. The difficulties in (v) (due to the fact that the material parameters vary in the rate of 10^{10}:

for mechanical stiffness c_{44}, 10 for the piezoelectric parameter e_{15} and for the dielectric parameters ε_{11} in the rate of 10^{-10}) are got over using functions Solve or FindInstance. The existing analytical solution of [14] for the homogeneous case FGPM helps for the validation of the BIEM solution.

5.2 Numerical results

The material used in the numerical examples is PZT-4, whose data are $c_{44}^0 = 2.56 \times 10^{10} N/m^2$, $e_{15}^0 = 12.7 C/m^2$, $\varepsilon_{11}^0 = 64.6 \times 10^{-10} C/Vm$ and $\rho^0 = 7.5 \times 10^3 kg/m^3$. The crack half-length is $c = 5mm$, it lies on the interval $(-c, c) \in Ox_1$ and is discretized by 5 BE. In the figures it is plotted the absolute value of the normalized SIF $K_{III}^* = \frac{K_{III}}{\tau\sqrt{\pi c}}$, $\tau = t_3^{in}$ versus normalized frequency $\Omega = c\sqrt{\rho^0/a_0}\omega$.

The validation study is presented in Figure 1 for the homogeneous PEM. The BIEM result is compared in with the result of [14]. It is observed that the maximum difference between both results obtained by different methods is about 7% - 10%.

In Figure 2 is given the BIEM solution for $rc = 0.2$, $\alpha = \pi/2$ and for $\alpha = 0$. In this case the critical value of the normalized frequency is $\Omega_0 = 0.2$ where a jump of the SIF appears. For $\Omega_0 > \Omega$ the dynamic behaviour is simple vibration, while for $\Omega_0 < \Omega$ the dynamic behaviour is wave propagation and the curve is similar to the homogeneous case in Figure 1. Also for $\alpha = 0$ the SIF at the left crack-tip is higher then at the right crack-tip, while for $\alpha = \pi/2$ the value of the SIF in both crack-tips is equal.

For $rc = 0.3$ and $\alpha = \pi/3$ it is presented the result for normalized SIF K_{III}^* in Figure 3. Again the jump of the SIF appear at the critical $\Omega_0 = 0.3$. It is observed that the maximum value of SIF on Figure 3 is less then the maximum value of SIF on Figure 2. Numerical examples show the depends on the magnitude r and on the direction α of the material inhomogeneity as well as the different behaviour of the SIF with respect to the critical value Ω_0.

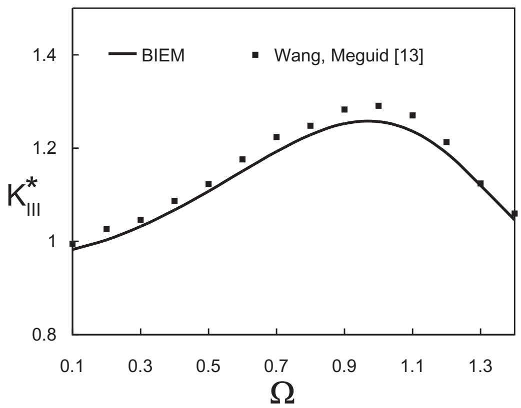

Figure 1: Normalized SIF K_{III} of a finite crack in a piezoelectric homogeneous plane.

6 Conclusions

Presented is numerical solution of integro-differential equations for anti-plane cracked FGPM. Using the derived with Radon transform fundamental solutions an efficient BIEM and a Mathematica program code is developed. Numerical examples for SIF computation

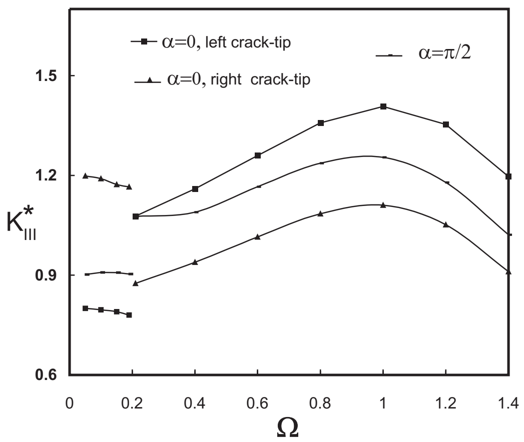

Figure 2: Normalized SIF K_{III} of a finite crack in a piezoelectric inhomogeneous plane, $rc = 0.2$

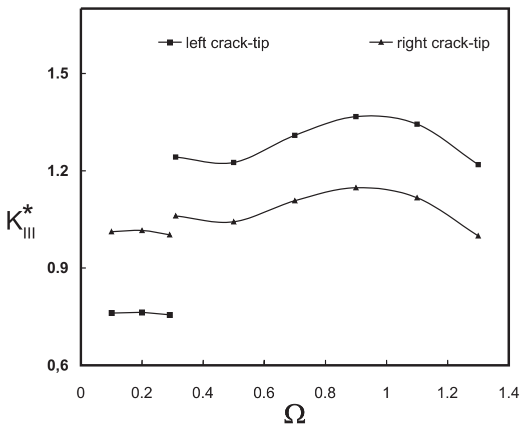

Figure 3: Normalized SIF K_{III} of a finite crack in a piezoelectric inhomogeneous plane, $rc = 0.3$.

are presented. The proposed methodology, numerical solution and program code can be applied for problems in non-destructive material testing as well as for solution of inverse problems in finite solids.

Acknowledgement The authors acknowledge the support of the Bulgarian NSF under the Grant No. DID 02/15.

REFERENCES

[1] M. Akamatsu, G. Nakamura. Well-Posedness of Initial-Boundary Value Problems for Piezoelectric Equations. *Appl. Anal.* 81, 129-141, 2002.

[2] H. Bateman and A. Erdelyi, Higher Transcendental Functions, McGraw-Hill, New York,1953.

[3] J. Chen, Zh. Liu, Zh. Zou. The central crack problem for functionally graded piezoelectric strip. *Int. J. Fracture* 121, 81-94, 2003.

[4] Y.S. Chan, G.H. Paulino, A.C. Fannjiang. The crack problem for nonhomogeneous materials under anti-plane shear loading-a displacement based formulation. *Int. J. Solids Struct.* 38, 2989-3005, 2001.

[5] C. H. Daros. On modelling SH-waves in a class of inhomogeneous anisotropic media via the Boundary Element Method. *ZAMM-Z. Angew. Math. Mech.* 90, 113-121, 2010.

[6] D. Gross, T. Rangelov, P. Dineva. 2D wave scatterig by a crack in a piezoelectric plane using traction BIEM. *J. Strct Integrity Durability,* 1(1):35-47, 2005.

[7] L.D. Landau, and E.M. Lifshitz, Electrodynamics of Continuous Media, Pergamon Press, Oxford 1960.

[8] C. Li, G. Weng. Antiplane crack problem in functionally graded piezoelectric materials. *J. Appl. Mech.(ASME)* **69**, 481-488, 2002.

[9] L. Ma, L.Z. Wu, Z.G. Zhou, L.C. Guo, L.P. Shi. Scattering of harmonic anti-plane shear waves by two collinear cracks in functionally graded piezoelectric materials. *Eur. J. Mech. A/Solid* 23, 633-643, 2004.

[10] T. Rangelov, P. Dineva. Dynamic behaviour of a cracked inhomogeneous piezoelectric solid. Part 2: anti-plane case. *C. R. Acad. Sci. Bulg.* 60:3, 231-238, 2007.

[11] T. Rangelov, P. Dineva, D. Gross. Effect of material inhomogeneity on the dynamic behavior of cracked piezoelectric solids: a BIEM approach. *ZAMM-Z. Angew. Math. Mech.* 88, 86-99, 2008.

[12] B.M. Singh, R.S. Dhaliwal, J. Vrbik. Scattering of anti-plane shear wave by an interface crack between two bonded dissimilar functionally graded piezoelectric materials. *Proc. R. Soc.* A 465, 1249-1269, 2009.

[13] V. Vladimirov, Equations of mathematical physics, Nauka, Moskow 1984.

[14] X.D. Wang, S.A. Meguid. Modelling and analysis of the dynamic behaviour of piezoelectric materials containing interfacing cracks. *Mech. Mater.* **32**, 723-737, 2000.

[15] C-Y. Wang, Ch. Zhang. 2D and 3D dynamic Green's functions and time-domain BIE formulations for piezoelectric solids. *Eng. Anal. Bound. Elem.*, **29**, 454-465, 2005

[16] A. Zayed, Handbook of Generalized Function Transformations, CRC Press, Boca Raton, Florida , 1996.